



REPORT ON CORRELATION PROCECURES

Submitted to:

**Office of Naval Research
875 North Randolph Street, Room 273
Arlington, VA 22203-1995**

**Dr. Paul Rispin, Program Manager
ONR Code 331
703.696.0339
rispinp@onr.navy.mil**

**In fulfillment of the requirements for:
Cooperative Agreement No. N00014-04-2-0003
*Agile Port and High Speed Ship Technologies***

**FY 05 Project 05-5
*Waterjet Self-Propulsion Model Test for Application to a High-Speed Sealift Ship***

Classification: Unclassified

Prepared and submitted by:

**Center for the Commercial Deployment of Transportation Technologies
California State University, Long Beach Foundation
6300 State University Drive, Suite 220 • Long Beach, CA 90815 • 562.985.7394**

January 17, 2007

DATA CORRELATION

**FY 05 PROJECT 05-6, PE 2.33
TASK NO. 5.6**

Data Correlation to Full Scale

System:

Data Correlation for Application to a High-Speed Sealift Ship
Utilizing Advanced Axial-Flow Waterjets

By:

CDI Marine Company
Systems Development Division
900 Ritchie Highway
Severna Park, MD 21146

For:

Center for the Commercial Deployment of Transportation Technologies
6300 State University Drive, Suite 220
Long Beach, CA 90815

CCDoTT Fiscal 2005 Subagreement: S07-305905CDI
Prime Agreement No.: N00014-04-2-0003
Task 5.6: Data Correlation

CCDoTT Project Director:
Stanley Wheatley
CCDoTT
6300 State University Drive, Suite 220
Long Beach, CA 90815

CDIM-SDD Technical Manager:
John Purnell
CDIM-SDD
900 Ritchie Highway, Suite 102
Severna Park, MD 21146

This material is based upon work supported by the Office of Naval Research, under Cooperative Agreement No N00014-04-2-0003 with the California State University, Long Beach Foundation, Center for the Commercial Deployment of Transportation Technologies, (CCDoTT).

Any opinions, findings, and conclusions or recommendations expressed in this material are those of the author(s) and do not necessarily reflect the views of the Center for the Commercial Deployment of Transportation Technologies (CCDoTT) at California State University, Long Beach.

FOREWORD

CDI Marine Systems Development Division (CDIM-SDD) prepared the work described in this Working Paper for the Center for the Commercial Deployment of Transportation Technologies (CCDoTT) at California State University, Long Beach. The principal point of contact at CDIM-SDD was Mr. John Purnell. The principal point of contact at CCDoTT was Mr. Stan Wheatley.

TABLE OF CONTENTS

	<u>PAGE</u>
1.0 Introduction	1
2.0 Background	1
3.0 Waterjet Scaling	2
3.1 Model and Ship Comparison.....	2
3.2 Flow Rate Scaling	2
4.0 Ship Resistance	4
5.0 CCDoTT Axial Waterjet Performance on the Ship.....	8
6.0 Discussion and Conclusions	9
7.0 References.....	10
Appendix A CCDoTT Axial Waterjet Performance Maps	

LIST OF FIGURES

	<u>PAGE</u>
1 Ship Inlet Wake Fractions as a Function of Flow Rate and Speed	3
2 Ship Thrust Deduction Factors as a Function of Ship Speed.....	7

LIST OF TABLES

	<u>PAGE</u>
1 Model and Ship Correlation Parameter Comparisons	2
2 Model and Ship Flow Conditions	4
3 Summary of Model to Ship Scaling Correlation Calculations	7
4 CCDoTT Axial Waterjet Design Point for the Ship.....	8

QUANTITIES AND SYMBOLS

Abbreviations	Definition	Units
Ca	Correction allowance	-----
Cf	Friction coefficient	-----
Cr	Form drag and wave resistance coefficient	-----
Ct	Total resistance coefficient	-----
g	Acceleration of gravity	feet/second ²
Head	Pump headrise	feet of water
IVR	Inlet velocity ratio	-----
JVR	Jet velocity ratio	-----
Lbf	Pounds force	pounds force
LWL	Waterline length	feet
N _{SSS}	Suction specific speed	-----
NPSH	Net positive suction head	feet of water
Patm	Atmospheric pressure	feet of water
Pnoz	Nozzle pressure	feet of water
Pvapor	Water vapor pressure	feet of water
Q _S	Ship waterjet pump flow rate	feet ³ /second
Q _{SP}	Self-propulsion model pump flow rate	feet ³ /second
R _{BH}	Bare hull resistance	-----
Rn	Reynolds number	-----
R _{RTF}	Revised tow force	pounds force
Rt	Total resistance	pounds force
R _{TF}	Conventional tow force	pounds force
RPM	Revolutions per second	1/sec
S	Wetted surface area	feet ²
SR	Scale ratio model to ship	-----
t	Thrust deduction factor	-----

T_{NET}	Waterjet net thrust	pounds force
U_{TIP}	Waterjet impeller tip speed	feet/second
V_{AX}	Waterjet average inlet face flow velocity	feet/second
V_{jet}	Jet momentum velocity	feet/second
V_M	Model speed	feet/second
V_S	Ship velocity	feet/second
w	Inlet wake fraction	-----
ΔC_f	Roughness allowance	-----
η_{WJ}	Waterjet hydraulic efficiency	-----
ρ	Water density	lbm/foot ³
ν	Kinematic viscosity	feet ² /second
ϕ	Flow coefficient, Phi	-----
ψ	Head coefficient, Psi	-----

Abbreviations

Definition

FW	Fresh Water
M	Model Scale
NSWCCD	Naval Surface Warfare Center, Carderock Division
S	Ship Scale
SR	Scale Ratio
SW	Sea Water
WJ	Waterjet

1.0 INTRODUCTION

Bare hull and self-propulsion model testing of a single catamaran-type side-hull with operating scaled waterjet inlets was performed at the Naval Surface Warfare Center, Carderock Division, on Towing Tank Carriage No 1. The objective of the 17.5-to-1 scale model tests was to take sufficient data to determine the inlet-hull interaction and determine the model waterjet self-propulsion conditions. This information could then be used for extrapolation and correlation to the full-scale ship, which would determine the full-scale waterjet flow and thrust requirement conditions. Different commercial waterjets are available, but the purpose is to demonstrate the sizing and performance of the CCDoTT axial-flow waterjet design in this ship. The CCDoTT axial waterjet design has been model tested separately in the water tunnel at NSWCCD. This information will be combined with the model hull derived data to determine the overall sizing and performance of the CCDoTT waterjet design.

2.0 BACKGROUND

Waterjet model testing is relatively new, and the body of test data and testing experience is a small fraction of the propeller database. The fundamentals of waterjet model testing have been the subject of a great deal of attention and study in recent years, and considerable progress has been made. The development of the momentum flux method of estimating powering characteristics and interaction effects has allowed waterjet model testing to be performed with much greater confidence than previously, and the database is expanding slowly but steadily. While the overall waterjet characterization capabilities remain somewhat limited relative to open water and towed model propeller testing, prediction techniques are improving rapidly. The waterjet inlets affect the flows and pressures on and around the aft portion of the hull, and continuing efforts to better understand what is occurring can only provide further benefits. This is the objective the tow tanks tests were aiming to support. The development of a database with a significant quantity of model to full-scale data correlations is a matter of importance in improving levels of confidence in predicting waterjet system performance.

Waterjets are of interest for many reasons for high-speed applications. The waterjet inlet will draw flow from the ship boundary layer region, which lowers the inlet momentum velocity of flow into the waterjet inlet to values below the ship speed. This lower momentum inlet flow improves the waterjet propulsive efficiency by recovering energy that would have been lost in the hull boundary layer. Waterjet flush inlets have very low drag impact on a ship, and for high-speed applications reducing drag is critical. Past model hull tests have indicated that negative thrust deduction factors are possible with waterjet propulsion systems installed¹. For comparison, typical propeller systems are always associated with a positive thrust deduction factor. Negative thrust deductions would be very desirable for high-speed shipping since this would mean that the waterjet system is actually lowering the drag of the ship compared to the bare hull drag of the same ship, which illustrates the importance of waterjet propulsion system development.

CCDoTT has supported a multi-phase effort to develop a large axial-flow waterjet design for application to high-speed shipping. Commercially available large waterjets have been based on mixed-flow pump designs, which result in a much heavier and wider waterjet system than an axial-flow waterjet system. Weight is a critical item on high-speed ships, therefore the benefit of a much lighter axial waterjet system is obvious. Since high speed favors narrow hulls with high length-to-beam ratios, there is a problem having enough transom width to install the requisite number of waterjet units to absorb the large amounts of power that can be required for high speed. If the transom must be widened to accommodate the waterjets, increased transom drag will result. The CCDoTT axial waterjet design is significantly narrower than a comparable mixed-flow design, and generally three axial waterjets can fit in the same transom width that could only accommodate two comparable mixed-flow waterjets. The need for axial-flow waterjets is obvious, and the effort reported herein looks at the sizing and performance impact of applying the CCDoTT axial waterjet design to a representative high-speed hull.

3.0 WATERJET SCALING

3.1 Model and Ship Comparison

The model was a 17.5-to-1 scaled ratio of a single representative catamaran-type hull. Most of the ship geometry and characteristics can be related with the scale ratio. The one difference is that the model is run in fresh water and the ship will be operated in seawater, and these properties must be accounted for. Table 1 gives essential comparisons needed for the proper correlation of the model data to the ship.

Table 1
Model and Ship Correlation Parameter Comparisons

	Model		Ship	
Waterline Length (feet)	LWL_M	19.8	LWL_S	346.5
Medium		Fresh Water		Seawater
Water Density (lb*sec ² /ft ⁴)	r_{FW}	1.937	r_{SW}	1.991
Kinematic Viscosity (ft ² /sec)	n_{FW}	1.07029E-05	n_{SW}	1.27909E-05
Wetted Surface Area (ft ²)	S_M	31.26	S_S	9573.38
Design Speed (knots)		9.562		40
Design Speed (feet per second)	V_M	16.139	V_S	67.51
Reynolds Number	Rn_M	2.9856E+07	Rn_S	1.8289E+09

3.2 Flow Rate Scaling

The model data established the self-propulsion flow rates, Q_{SP} , and the jet velocity ratios, JVR , for the different model speeds, V_M , where:

$$JVR = \frac{V_{jet}}{V_M} \quad (1)$$

The model self-propulsion flow rates are scaled to the ship flow rates, Q_S , by the 17.5 scale ratio, SR , between the model and the ship raised to the 2.5 power, where:

$$Q_S = Q_{SP} * (Scale\ Ratio)^{2.5} \quad (2)$$

The model JVR at the self-propulsion points is the same as the ship JVR at the corresponding scaled ship speeds. With the ship's waterjet flow rates known, a revised inlet momentum velocity for the ship is needed because of the difference in boundary layers between the model and the ship. The lower Reynolds number of the model boundary layer results in a proportionately thicker boundary layer on the model, which results in larger values for the inlet wake fraction, w_M , on the model. For the ship, the model boundary layer profile is scaled based on the increase in Reynolds number^{2,3}, and the ship inlet wake fractions, w_S , can be calculated from programming for the ship flow rates using a comparable capture shape profile to that used for the model. The programming will integrate the revised ship boundary layer profiles with the capture shape to determine a capture height that satisfies the ship flow rate, which then establishes the inlet momentum velocity for the ship inlet flow condition. Figure 1 shows the ship inlet wake fractions as a function of ship speed and flow rates from the calculation.

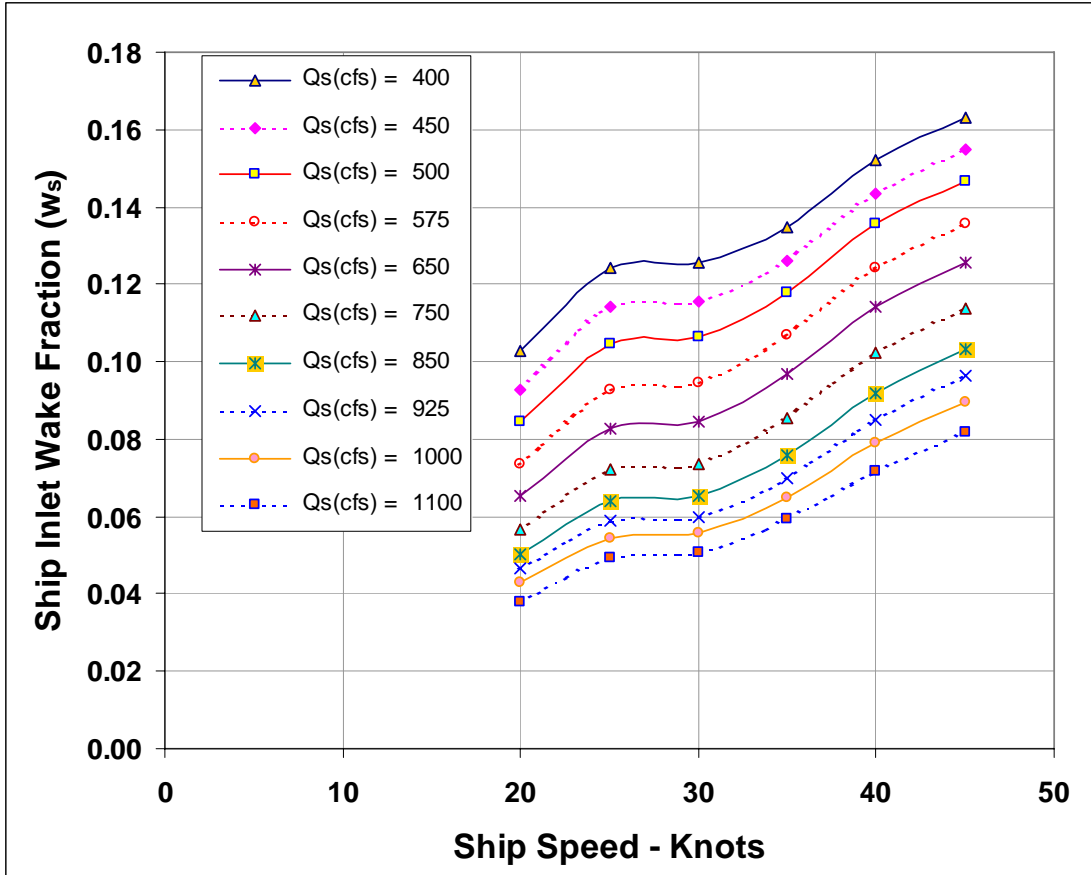


Figure 1. Ship Inlet Wake Fractions as a Function of Flow Rate and Speed

With the ship inlet wake fractions determined, the net thrust from the ship waterjets can be calculated for each speed from:

$$T_{NET} = \rho_{SW} * Q_S * V_S * (JVR - (1 - w_s)) * (Number\ of\ Waterjets) \quad (3)$$

Table 2 summarizes the flow rates and inlet wake fractions for the model and ship, with the ship net thrust from the two waterjets, calculated from Equation 3, also shown. The ship net waterjet thrust shown is the thrust that is required to propel the ship at each speed based on the scaled model test results. This thrust data will be compared with the ship total resistance, determined from scaling of the model bare hull resistance, to determine the ship thrust deduction factor, t_s .

Table 2
Model and Ship Flow Conditions

Model Speed #	Ship Speed V_S (knots)	Model Speed V_M (fps)	Self-Propulsion Flow Rate per Pump Q_{SP} (cfs)	Model Inlet Wake Fraction w_M	Jet Velocity Ratio JVR	Ship Flow Rate per Pump Q_S (cfs)	Ship Inlet Wake Fraction w_S	Ship Waterjet Net Thrust with Both Pumps T_{NET} (lbf)
8	20	8.07	0.3606	0.1778	1.7910	461.95	0.0908	54753.7
10	25	10.09	0.4312	0.1857	1.7117	552.40	0.0962	74984.6
12	30	12.10	0.5051	0.1703	1.6695	647.10	0.0850	98445.1
14	35	14.12	0.5672	0.1695	1.6062	726.72	0.0879	118651.8
16	40	16.14	0.6258	0.1819	1.5497	801.74	0.0966	139312.8
18	45	18.16	0.6895	0.1865	1.5171	883.35	0.1002	164917.3

4.0 SHIP RESISTANCE

Procedures for scaling the model resistance to the ship resistance have been developed by model testers based on long experience. Reynolds number, Rn_M and Rn_S , for the model and the ship, respectively, is an important scaling parameter and it is determined by:

$$Rn_M = \frac{V_M * LWL_M}{V_{FW}} \quad (4)$$

for the model, and for the ship by:

$$Rn_S = \frac{V_S * LWL_S}{V_{SW}} = \frac{V_M * LWL_M * SR^{1.5}}{V_{SW}} \quad (5)$$

At the low Reynolds numbers of the model, the frictional resistance will be proportionately much greater than for the ship, and this is accounted for by using the frictional coefficients, Cf_M and Cf_S , for the model and the ship, respectively. The frictional coefficients are based on the International Towing Tank Conference (ITTC) friction line equation⁴:

$$Cf_M = \frac{0.075}{(\log_{10} Rn_M - 2)^2} \quad (6)$$

for the model, and for the ship by:

$$Cf_S = \frac{0.075}{(\log_{10} Rn_S - 2)^2} \quad (7)$$

A correlation allowance, Ca , which typically ranges from +0.0004 to -0.0002, is set by experience to account for additional scale effects in order to get a better prediction of the full-scale results where, for this case:

$$Ca = 0.00017 \quad (8)$$

Because of the difference in primarily frictional terms between the model and the ship, a roughness allowance, ΔC_f , is needed for the scaling, where:

$$\Delta C_f = C_{f_M} - C_{f_S} - Ca \quad (9)$$

The ΔC_f is used to calculate the conventional towing force, R_{TF} , that is typically applied to towed models to account for primarily the frictional difference between model and ship based on the model wetted surface, S_M , where:

$$R_{TF} = \frac{\rho_{FW}}{2} * \Delta C_f * V_M^2 * S_M \quad (10)$$

As an extension of this for waterjet testing, Hoyt, in Reference 5, used a revised tow force, R_{RTF} , that is used to determine the waterjet self-propulsion operating conditions due to the fact that the waterjet will ingest portions of the hull boundary layer, which benefit the waterjet thrust, but would not be properly accounted for using only the conventional tow force:

$$R_{RTF} = R_{TF} * \left(\frac{C_{f_M}}{C_{f_S}} - 1 \right) \quad (11)$$

The model total resistance coefficient, C_{t_M} , is determined from the model bare hull drags, R_{BH} , that were measured at each model speed by:

$$C_{t_M} = \frac{R_{BH}}{0.5 * \rho_{FW} * V_M^2 * S_M} \quad (12)$$

The form drag and wave resistance of the model are grouped as a single coefficient, C_{r_M} , and are considered as functions of Froude number only so that:

$$C_{r_M} = C_{t_M} - C_{f_M} \quad (13)$$

Since the comparable model and ship speed conditions are at the same Froude number, the ship form drag and wave resistance coefficient, C_{r_S} , will have the same value as the model:

$$C_{r_S} = C_{r_M} \quad (14)$$

The ship total resistance coefficient, C_{t_S} , is then found from:

$$C_{t_S} = C_{f_S} + C_{r_S} + Ca \quad (15)$$

The ship total resistance, Rt_S , is then determined from:

$$Rt_S = \frac{\rho_{SW}}{2} * Ct_S * V_S^2 * S_S \quad (16)$$

where S_S is the ship wetted surface, which can be scaled from the model wetted surface area by:

$$S_S = S_M * (Scale\ Ratio)^2 \quad (17)$$

The ship total resistance is compared with the ship waterjet net thrust requirement to determine the ship thrust deduction factor, t_S , by:

$$t_S = 1 - \frac{Rt_S}{T_{NET}} \quad (18)$$

The results of the above sequence of calculations at each speed are summarized in Table 3, with the resulting ship thrust deduction factors listed on the bottom table line and also plotted on Figure 2 versus ship speed. The 40-knot ship speed is the design point speed, and the thrust deduction is minimum and negative in that region. The negative thrust deductions indicate that the waterjet propulsion system actually acts to reduce the basic ship total resistance at the design speed and other conditions. Negative thrust deduction is desirable and is something that does not occur with typical propeller-driven ships. The impact of negative thrust deduction with waterjet-propelled ships is a very strong incentive for continued development and understanding of waterjet systems for application to high-speed ships.

Table 3

Summary of Model to Ship Scaling Correlation Calculations

Froude Number	0.320	0.400	0.480	0.560	0.639	0.719
Model Speed, V_M , fps	8.07	10.09	12.10	14.12	16.14	18.16
Ship Speed, V_S , knots	20	25	30	35	40	45
Model Total Resistance, R_{tM} , Lbf	11.72	16.82	22.31	27.98	33.63	39.09
Reynolds Number, Rn_M	1.479E+07	1.849E+07	2.219E+07	2.589E+07	2.959E+07	3.329E+07
Friction Coefficient, Cf_M	2.806E-03	2.704E-03	2.624E-03	2.560E-03	2.506E-03	2.459E-03
Reynolds Number, Rn_S	9.152E+08	1.144E+09	1.373E+09	1.602E+09	1.830E+09	2.059E+09
Friction Coefficient, Cf_S	1.548E-03	1.505E-03	1.472E-03	1.445E-03	1.422E-03	1.402E-03
Correlation Allowance, Ca	1.70E-04	1.70E-04	1.70E-04	1.70E-04	1.70E-04	1.70E-04
$D Cf = Cf_M - Cf_S - Ca$	1.088E-03	1.028E-03	9.819E-04	9.446E-04	9.137E-04	8.873E-04
Conventional Tow Force, R_{TF} , Lbf	2.145	3.167	4.355	5.703	7.204	8.855
$(Cf_M / Cf_S - 1)$	0.813	0.796	0.782	0.771	0.762	0.754
$R_{RTF} = R_{TF} * (Cf_M / Cf_S - 1)$, Lbf	1.744	2.521	3.408	4.399	5.490	6.677
Model Total Resistance Coefficient, Ct_M	5.945E-03	5.462E-03	5.029E-03	4.634E-03	4.265E-03	3.917E-03
Model Form Drag & Wave Resistance Coefficient, $Cr_M = Ct_M - Cf_M$	3.139E-03	2.758E-03	2.405E-03	2.074E-03	1.760E-03	1.457E-03
$Cr_S = Cr_M$	3.139E-03	2.758E-03	2.405E-03	2.074E-03	1.760E-03	1.457E-03
Ship Total Resistance Coefficient $Ct_S = Cf_S + Cr_S + Ca$	4.857E-03	4.433E-03	4.047E-03	3.689E-03	3.352E-03	3.029E-03
Ship Total Resistance, R_{tS} , Lbf	52741.7	75227.4	98891.4	122695.8	145595.0	166538.2
Total Ship Waterjet Net Thrust, T_{net} , Lbf	54753.7	74984.6	98445.1	118651.8	139312.8	164917.3
Ship Thrust Deduction Factor, $t_S = 1 - R_{tS} / T_{NET}$	0.0367	-0.0032	-0.0045	-0.0341	-0.0451	-0.0098

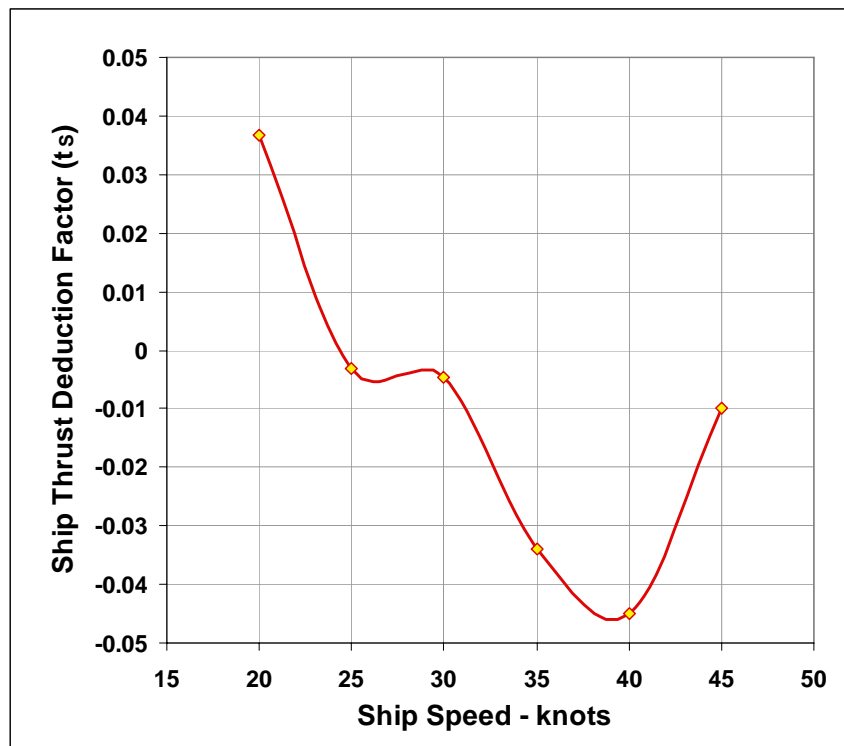


Figure 2. Ship Thrust Deduction Factors as a Function of Ship Speed

5.0 CCDoTT AXIAL WATERJET PERFORMANCE ON THE SHIP

The CCDoTT axial waterjet that was developed and model tested under earlier phases^{6,7} of this CCDoTT effort will be evaluated for use on the ship based on results from the model tests. The CCDoTT axial waterjet pump design is a true axial pump design, with the impeller and stator maximum diameters no greater than the inlet diameter to the waterjet since the design does not rely on radial components of flow for any of its headrise such as is done with mixed-flow pumps. This enables a more compact and lighter weight waterjet system, which is of importance to high-speed shipping. The CCDoTT axial waterjet design was characterized during its model testing⁷ to obtain the two nondimensional terms, flow coefficient, ϕ , and head coefficient, ψ , at its design point where:

$$\phi = \frac{V_{AX}}{U_{TIP}} = 0.375 \quad (19)$$

and:

$$\psi = \frac{2 * g * Head}{U_{TIP}^2} = 0.464 \quad (20)$$

Equations 19 and 20 include the design point values for the flow and head coefficients that were determined from the earlier testing of the CCDoTT axial waterjet pump in the water tunnel at NSWCCD⁷. Equation 21 gives the minimum expected scaled waterjet pump hydraulic efficiency, η_{WJ} , from those tests:

$$\eta_{WJ} = 0.918 \quad (21)$$

The head and flow coefficients can be used to scale and apply the CCDoTT axial waterjet pump design to any ship speed and power condition of interest. The available power for each waterjet pump was kept at 12,069 horsepower for this 40-knot design point where each pump needs to produce 69,656 pounds of net thrust, as shown in Table 2. Each waterjet needs to have a flow rate of $Q_S = 801.74$ cubic feet per second with a waterjet jet velocity ratio of $JVR = 1.55$ at the 40-knot design point conditions, also shown in Table 2. Matching the required operating point is an iterative process that requires accounting for the many variables, including inlet losses, and has been computerized with the inputs and resulting matching design point conditions shown in Table 4.

Table 4
CCDoTT Axial Waterjet Design Point for the Ship

Original CCDoTT design point Phi & Psi															
PUMP : Fixed			INPUTS :							Calculated or Fixed Values :					
Utip (fps)	Psi	Phi	Vdesign	Inlet	Pump	Pump	Nozzle	Power	Trans	WJ Shaft	Patm	Pvapor	Lamda	Sea Water	
Increment	Head Coef	Flow Coef	knots	Wake	Effic	Depth-ft	Depth-ft	HP	Eff	HP	feet	feet	Hub/Tip	lbm/ft ³	
0.01	0.464	0.375	40	0.0966	0.918	3.2	0	12069	1.000	12069	33.1	0.81	0.3	64.06	
Tip Speed	Vax	Head	Flow	Diameter	RPM	IVR	Ram	NPSH	Nsss	Pnoz	Vjet	JVR	Nozzle	Net Thrust	Propulsive
fps	fps	ft	cfs	inch		Ratio	Recovery	ft		ft	fps		Ratio	lbf	Efficiency
128.275	48.10	118.65	801.74	57.949	507.32	0.7555	0.8351	83.77	10991	170.12	104.63	1.550	0.6468	69,656	0.7085

The resulting waterjet pump has a maximum diameter of 57.95 inches at an operating speed of 507.3 RPM. The waterjet pump was assumed to have a minimum design point operating depth of 3.2 feet based on the model trim data with a ventilated transom at the design speed. The suction specific speed of this waterjet will be $N_{sss} = 10,991$, which is at least 15 percent below the minimum cavitation inception

value for this waterjet based on the previous water tunnel tests of the pump⁷. The propulsive efficiency for the CCDoTT axial waterjet installed on this ship would be 70.85 percent, with the expected inlet wake fraction of $w_S = 0.0966$ and the ship thrust deduction of $t_S = -0.0451$, based on the scaling of the self-propulsion model tests.

Axial waterjet systems are at least 15 to 20 percent lighter than comparable mixed-flow waterjet systems, even for the same inlet diameter. However, the CCDoTT axial pump is almost 2 percent smaller in inlet diameter than would be expected for a potential alternative mixed-flow waterjet installation, which further benefits the use of axial-flow waterjet designs. Also, since waterjet system weight varies on the order of the cube of inlet diameter, this translates into a very meaningful (5.5 percent) additional weight savings for a high-speed ship from even this modest reduction in diameter.

The above CCDoTT axial waterjet design was run through the CDIM waterjet off-design performance computer program. The off-design program calculates the expected waterjet system performance at speeds and power other than for the 40-knot design point condition. Appendix A shows the resulting performance maps for the proposed waterjet system as a function of ship speed and applied power for a large range of variables of interest. The required waterjet thrusts from Table 2 are equal to the ship drag and were plotted on the thrust maps in Appendix A. A loadline that varied with the ship speed to the 4/3 power provided a very close approximation to the drag curve. A loadline for one pump or both pumps operating is shown on most of the maps to indicate where the waterjet would be expected to operate under most conditions. The single pump loadline would represent the case where one of the two waterjets is not operating or is shut down due to problems. Of interest is the suction specific speed plot with single pump operation that indicates that the single CCDoTT axial waterjet could operate at full power without cavitation breakdown, which would not occur before reaching suction specific speeds (N_{SS}) of 14,000 or more, as was shown by the pump loop tests⁷.

6.0 DISCUSSION AND CONCLUSIONS

The model of the single catamaran-type hull was tested to determine model self-propulsion points with operating model waterjets. The model resistance data and the model waterjet pump self-propulsion operating data were scaled for the full-scale ship case. The model results established the requisite self-propulsion flow rates and jet velocity ratios that were required for the model. This established waterjet system performance requirements for the ship. The model boundary layer data was scaled to the ship size using Reynolds number scaling procedures. The ship boundary layer was then integrated with an appropriate capture shape profile to establish the base capture height that meets the waterjet flow requirement. This also established the inlet momentum value for the flow, which is needed as part of the ship waterjet net thrust calculations. The model total resistance data was scaled to determine the ship total resistance using the scaling procedures that were described. The comparison of the ship total resistance with the waterjet net thrust determined the thrust deduction factors for the ship.

The results indicated that at the 40-knot ship design point, the ship waterjets would have an inlet wake fraction of $w_S = 0.0966$ while operating at a jet velocity ratio, JVR, of about 1.55 with a flow rate of 801.74 cubic feet per second per pump. The total required net thrust from both waterjets was $T_{NET} = 139,313$ pounds force, while the scaled ship total resistance was $Rt_S = 145,595$ pounds force. This resulted in a 40-knot design point thrust deduction factor of $t_S = -0.0451$. The thrust deduction factor was negative for ship speeds in the 25 to 45-knot range, and was at its minimum in the 40-knot design point speed region. Negative thrust deduction factors are significant as they indicate that the presence of the waterjet system helps reduce drag compared to the baseline bare hull drag. Negative thrust deductions are most often unheard of for typical propeller-driven ships. The waterjet system, with its low-drag flush inlet and its favorable influence on the hull pressures, will be important for high-speed ship applications.

The CCDoTT axial waterjet pump was evaluated for its sizing and performance in this representative high-speed ship hull application. A model of the CCDoTT axial waterjet pump had been tested separately in the water tunnel at NSWCCD to establish its performance characteristics⁷. Combining the water tunnel pump results with the present scaled model hull results will establish the sizing and performance for a CCDoTT axial waterjet installation. The water tunnel tests established the design point head and flow

coefficients for the CCDoTT axial pump design and indicated a pump hydraulic efficiency of no less than 91.8 percent. This information enables the axial waterjets to be scaled to any craft speed and power application of interest using programming that accounts for the other waterjet system considerations such as inlet losses. The present representative ship design was based on having 12,069 horsepower available for each waterjet at the 40-knot design speed. The resulting CCDoTT axial waterjet for this application had an inlet and impeller diameter of 57.95 inches and operated at 507.3 RPM to produce the required net thrust at 40 knots from a flow rate of $Q_S = 801.74$ cubic feet per second per pump and a jet velocity ratio of $JVR = 1.55$. The propulsive efficiency for the CCDoTT axial waterjet installation with this ship will be 70.85 percent. The axial waterjets have a suction specific speed of $N_{SSS} = 10,991$ at the 40-knot design point speed, which is at least 15 percent below their cavitation inception value from the water tunnel testing. Off-design predictions showed that with only one axial waterjet operating instead of two, the single axial waterjet could still absorb full power with N_{SSS} of less than 14,000, while exceeding the N_{SSS} 14,000 to 14,500 range would increasingly likely cause cavitation breakdown based upon the water tunnel test results.

Axial waterjet units have a 15-20 percent weight advantage over comparable mixed-flow designs because of their straight-through flow design, which does not require any radial growth that adds weight. Also, this gives axial waterjets a narrower installation width, which allows more units to be installed in the limited transom widths favored for high-speed craft. In addition, the inlet diameter of the CCDoTT design is about 2 percent smaller than proposed alternative waterjets for the application which are based on mixed-flow pump designs rather than the more compact axial-flow design. The smaller inlet diameter requirements of the axial-flow design also save system weight since weight varies as approximately the cube of diameter, and even small reductions in diameter can provide meaningful weight savings, especially on large, high-powered waterjets.

7.0 REFERENCES

- 1) Wilson, M.B., S. Gowing, C.J. Chesnakas, and C.W. Lin, "Waterjet-Hull Interactions for Sealift Ships", ICMRT Conference, Ischia Porto, Italy, 19-21 September 2005.
- 2) Purnell, J G, "The Performance Gains of Using Wide, Flush Boundary Layer Inlets on Waterjet Propelled Craft", DTNSRDC Report PAS-75-45, March 1976.
- 3) Wilson, M.B. et al., "Analysis Of Hull Boundary Layer Velocity Distributions With And Without Active Waterjet Inlets" RINA Waterjet Propulsion IV, London, England 26-27 May 2004.
- 4) Proceedings of the 8th ITTC, Madrid, Spain 1957, published by Canal de Experiencias Hidrodinamicas, El Pardo, Madrid.
- 5) "Development of Design Technology for Integrated Waterjet Inlets, Nozzles, and Hullforms", CDIM-SDD Final Report for GCRMTC Research Project No. AMTC99-113, February 2003.
- 6) "Development Of A High-Speed Sealift Waterjet Propulsion System", CDIM-SDD Final Report No 748-9 prepared for The Center for Commercial Deployment of Transportation Technology, CCDoTT, September 2003.
- 7) "Model Test and Evaluation of an Advanced Axial-Flow Waterjet Pump", Final Report No 790-9 prepared for The Center for Commercial Deployment of Transportation Technology, CCDoTT, July 2005.
- 8) CDI Marine System Development Division Report, WP 748-2, "System Trade-Off Analysis to Select the Most Promising Waterjet propulsion System", September 2003.

APPENDIX A

CCDoTT Axial Waterjet Performance Maps

LIST OF FIGURES

		<u>PAGE</u>
A1	Waterjet Net Thrust Map per Pump versus Speed and Power.....	A-3
A2	Net Waterjet Thrust Map of Both Pumps versus Speed and Power.....	A-3
A3	Waterjet RPM Map as a Function of Speed and Power	A-4
A4	Map of Waterjet Torque per Pump versus Speed and Power	A-4
A5	Waterjet Headrise Map as a Function of Speed and Power.....	A-5
A6	Map of Flow Rate per Pump versus Speed and Power.....	A-5
A7	Map of Waterjet Net Positive Suction Head versus Speed and Power	A-6
A8	Map of Suction Specific Speed for the Waterjet versus Speed and Power.....	A-6
A9	Waterjet Pump Efficiency Map versus Speed and Power	A-7
A10	Propulsive Efficiency Map as a Function of Speed and Power	A-7
A11	Inlet Loss Coefficient Map versus Speed and Power	A-8
A12	Inlet Velocity Ratio Map versus Speed and Power.....	A-8
A13	Waterjet Jet Velocity Ratio Map as a Function of Speed and Power	A-9

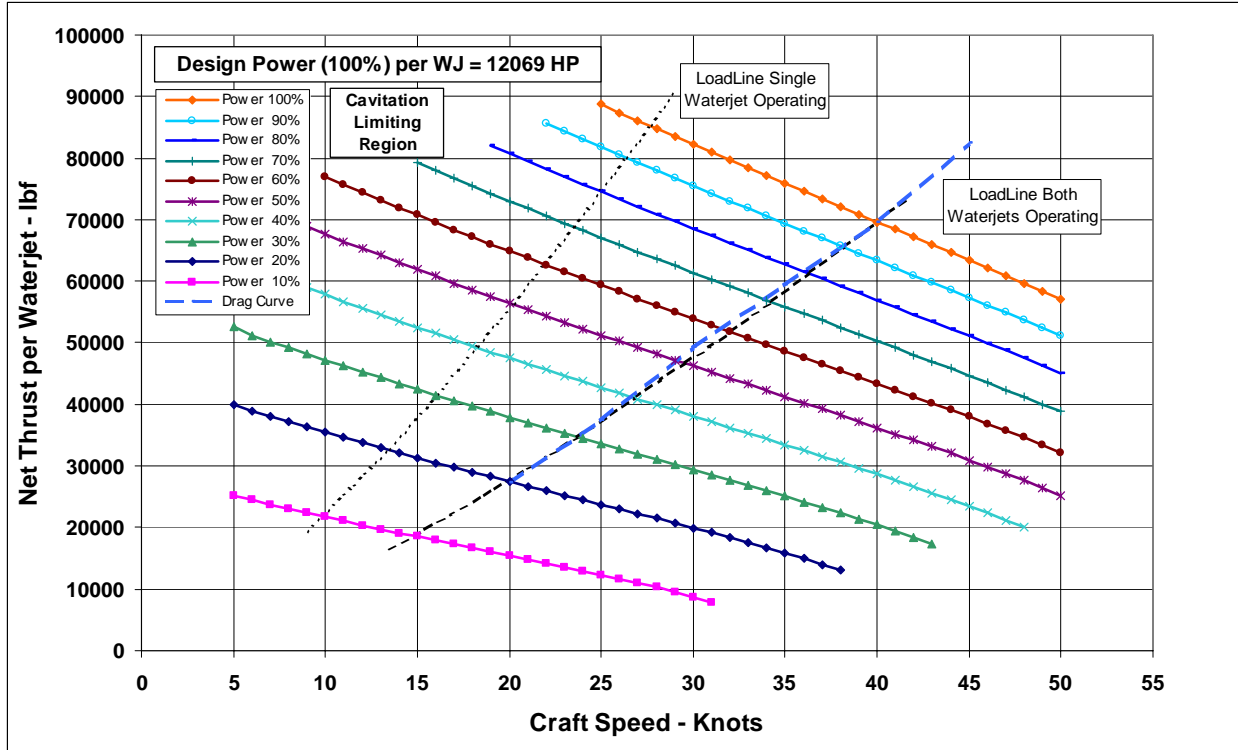


Figure A1. Waterjet Net Thrust Map per Pump versus Speed and Power

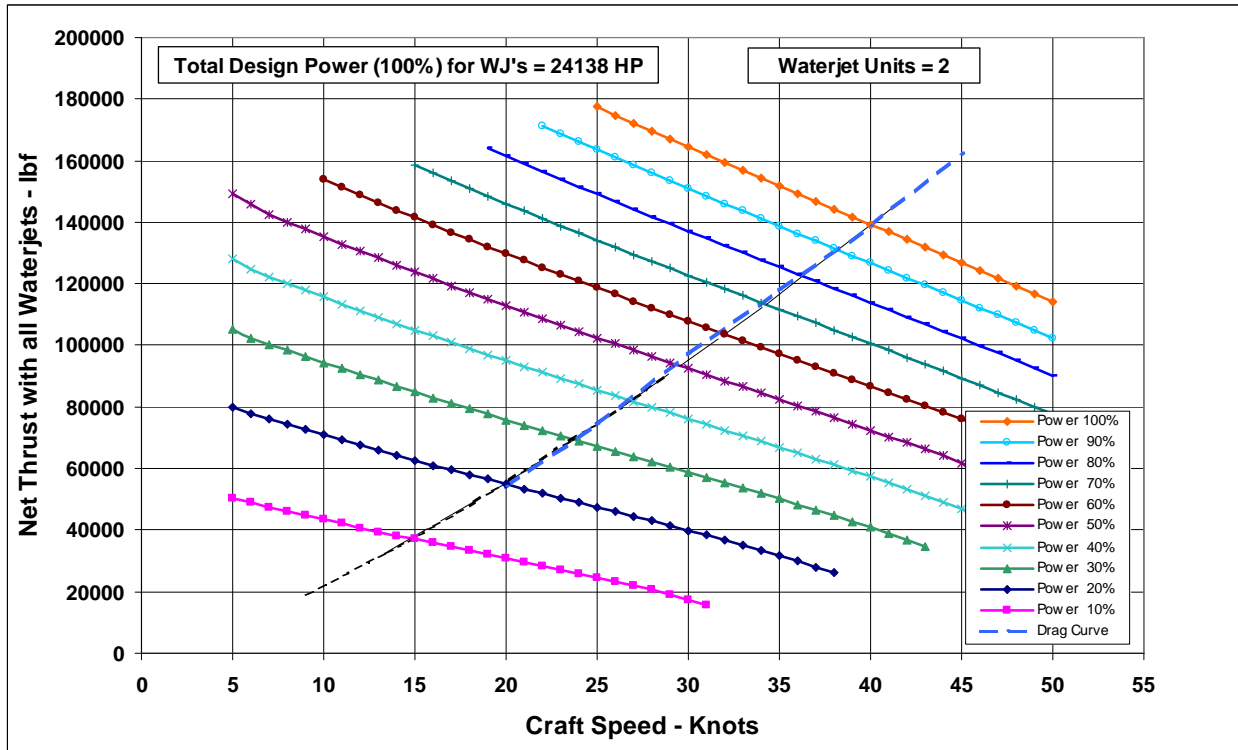


Figure A2. Net Waterjet Thrust Map of Both Pumps versus Speed and Power

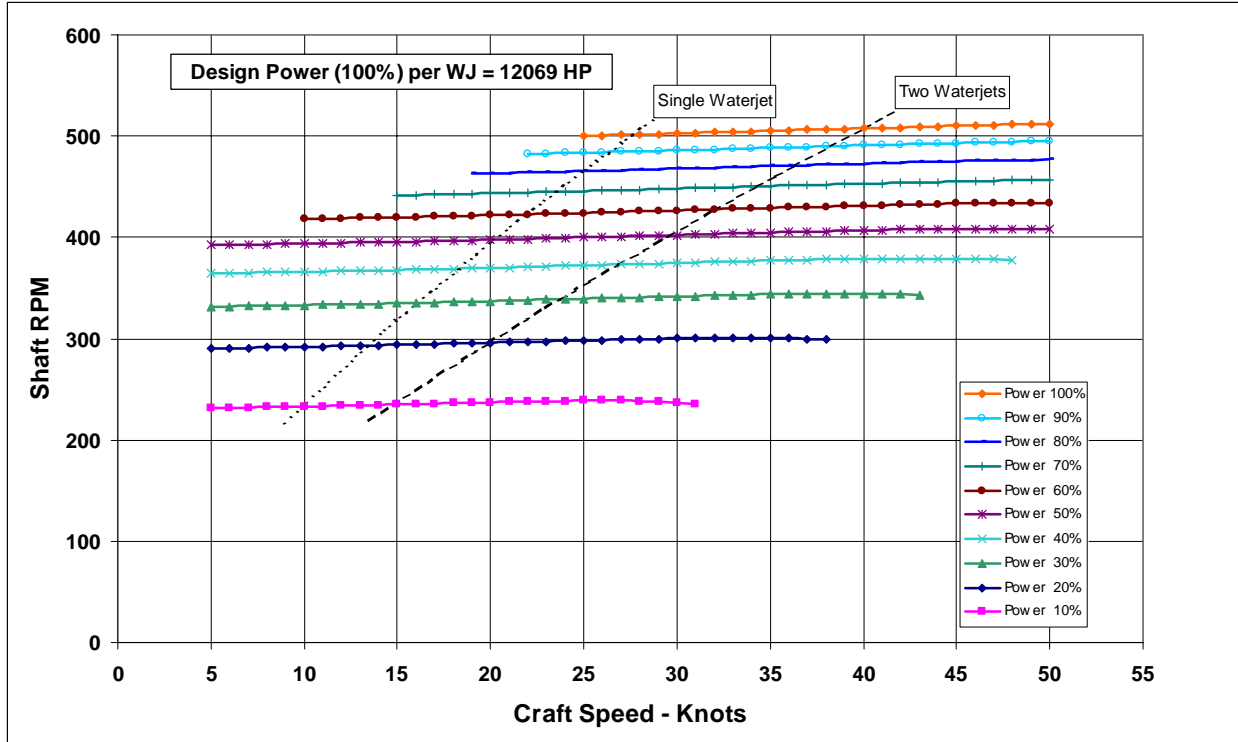


Figure A3. Waterjet RPM Map as a Function of Speed and Power

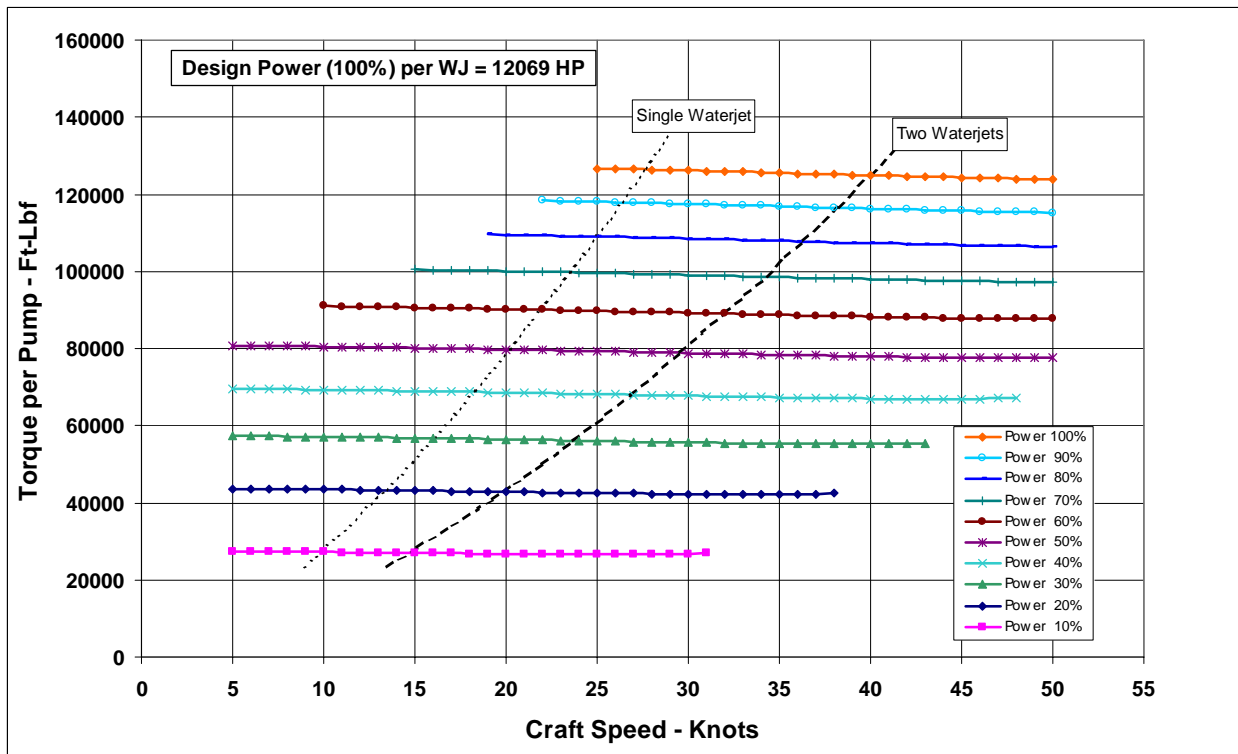


Figure A4. Map of Waterjet Torque per Pump versus Speed and Power

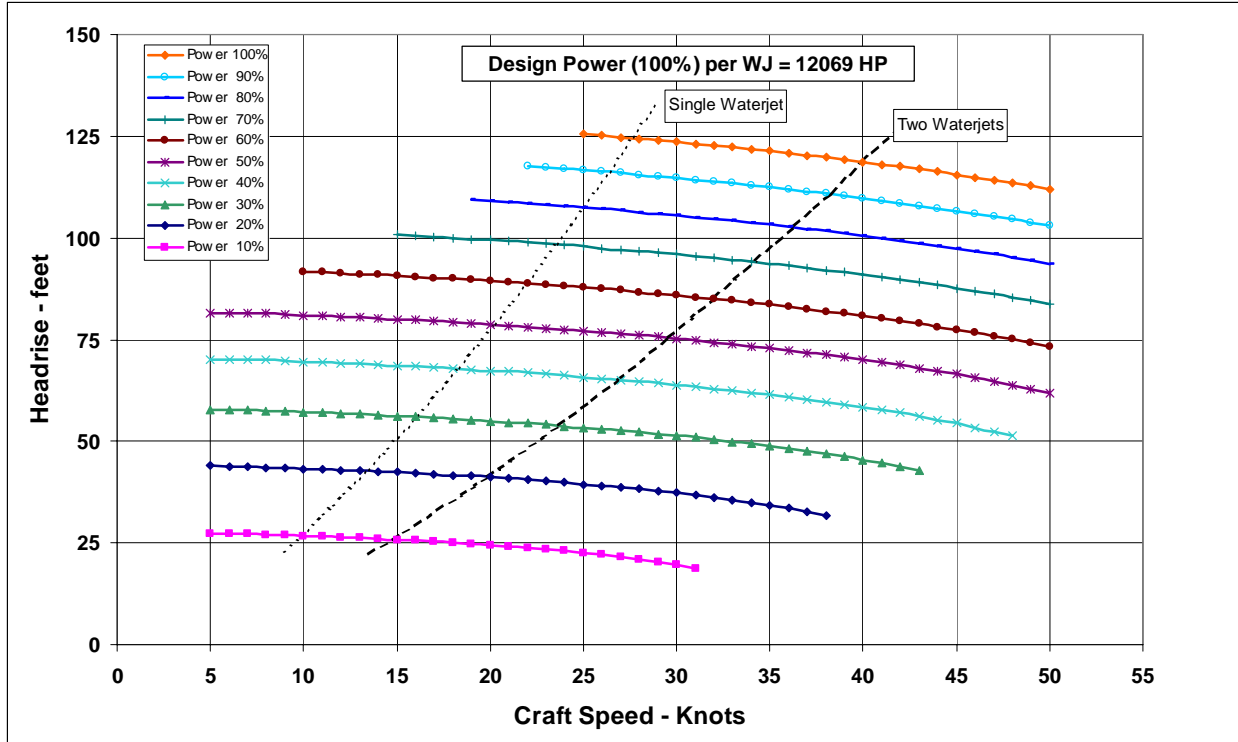


Figure A5. Waterjet Headrise Map as a Function of Speed and Power

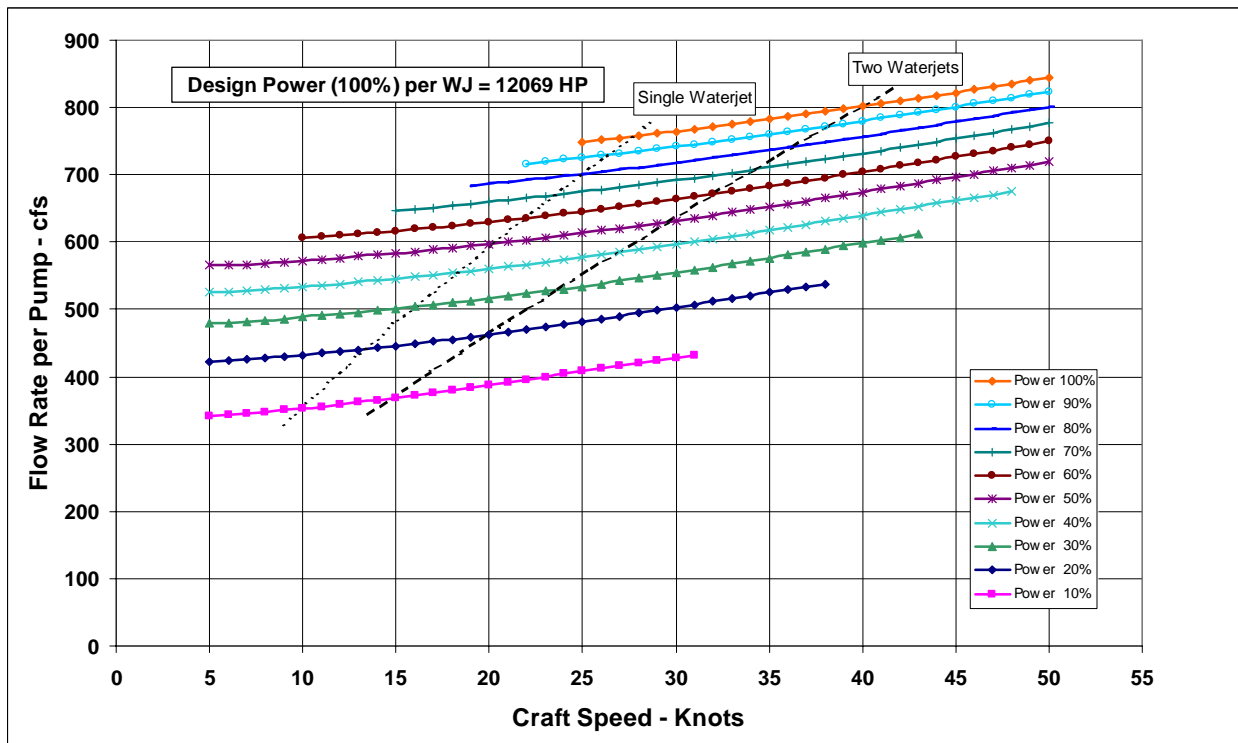


Figure A6. Map of Flow Rate per Pump versus Speed and Power

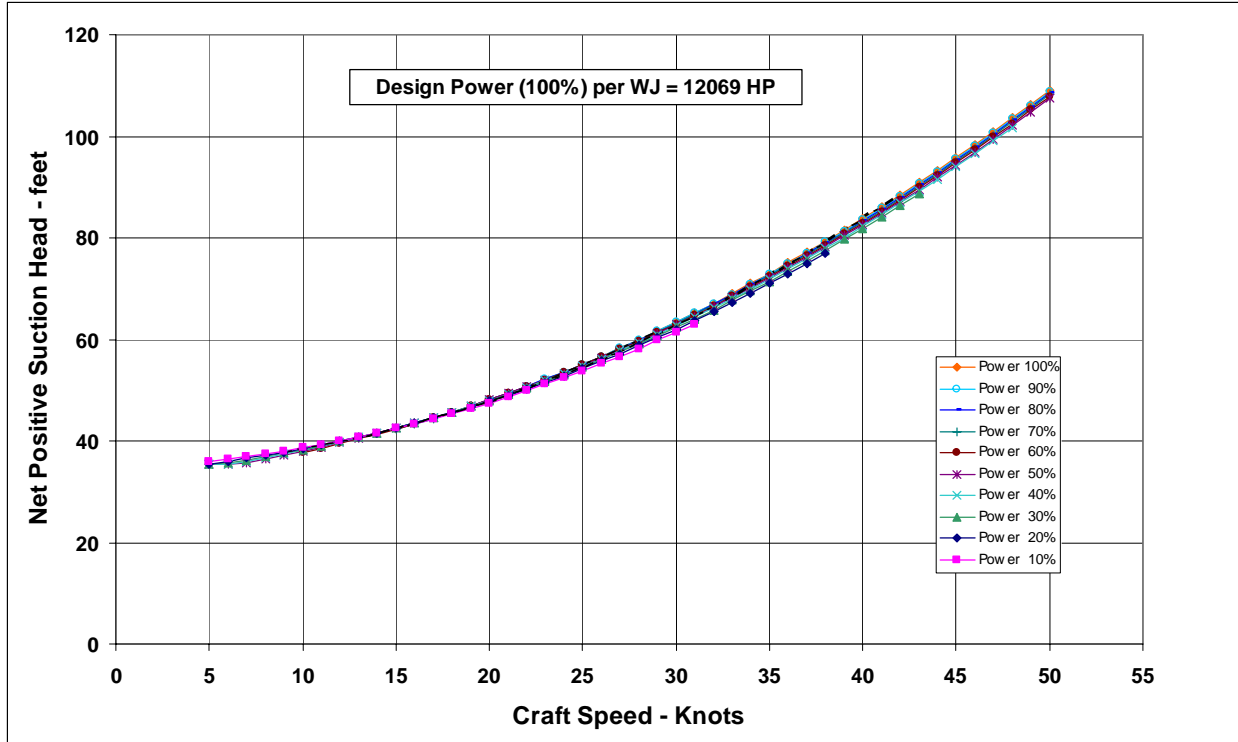


Figure A7. Map of Waterjet Net Positive Suction Head versus Speed and Power

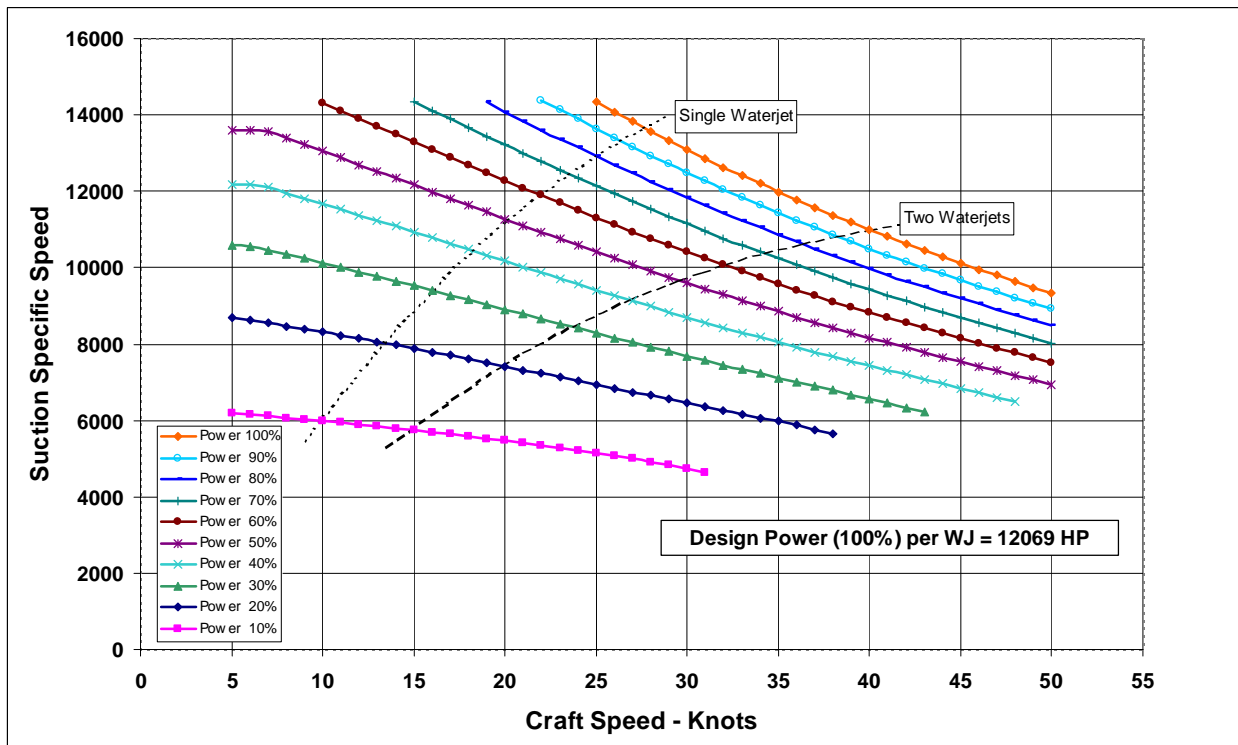


Figure A8. Map of Suction Specific Speed for the Waterjet versus Speed and Power

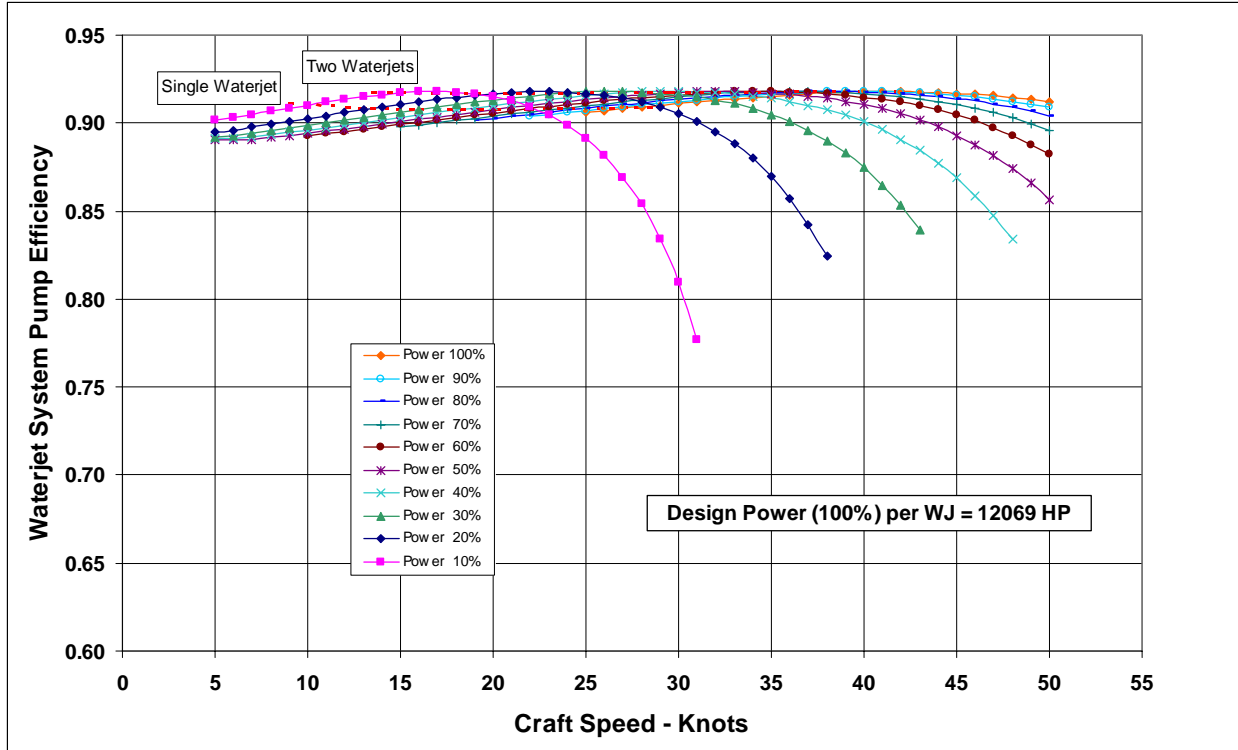


Figure A9. Waterjet Pump Efficiency Map versus Speed and Power

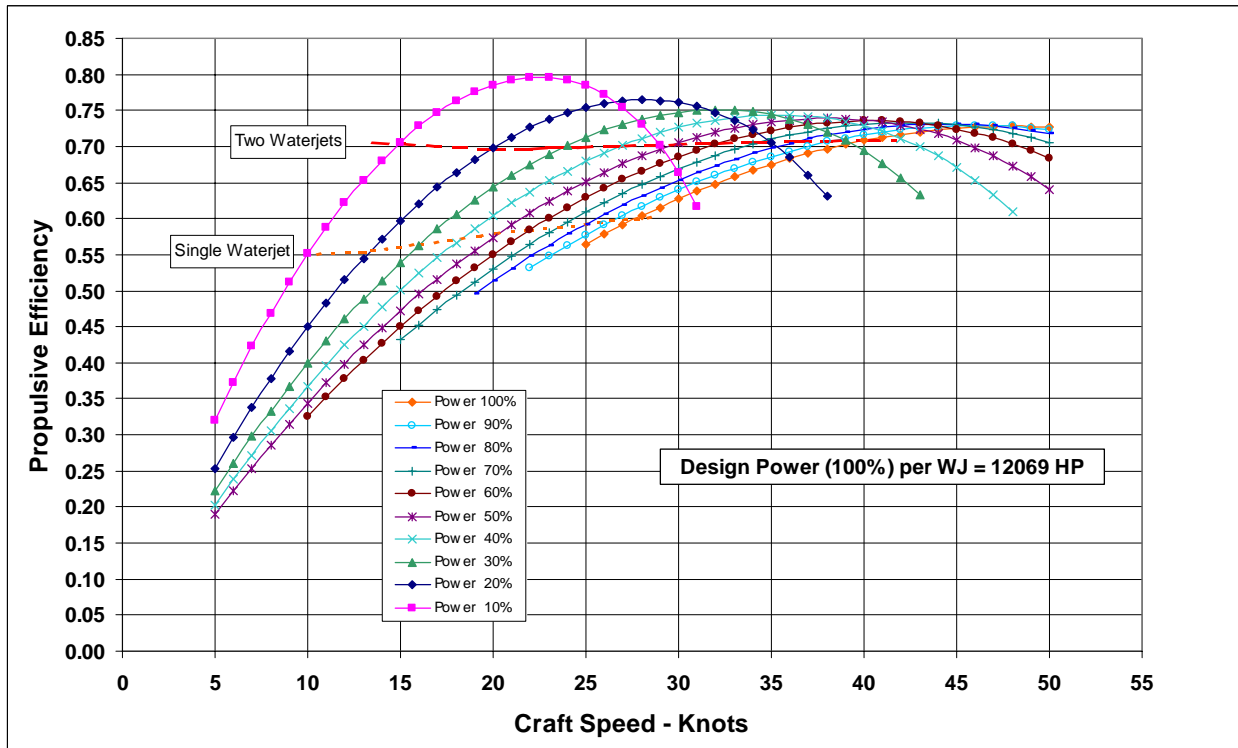


Figure A10. Propulsive Efficiency Map as a Function of Speed and Power

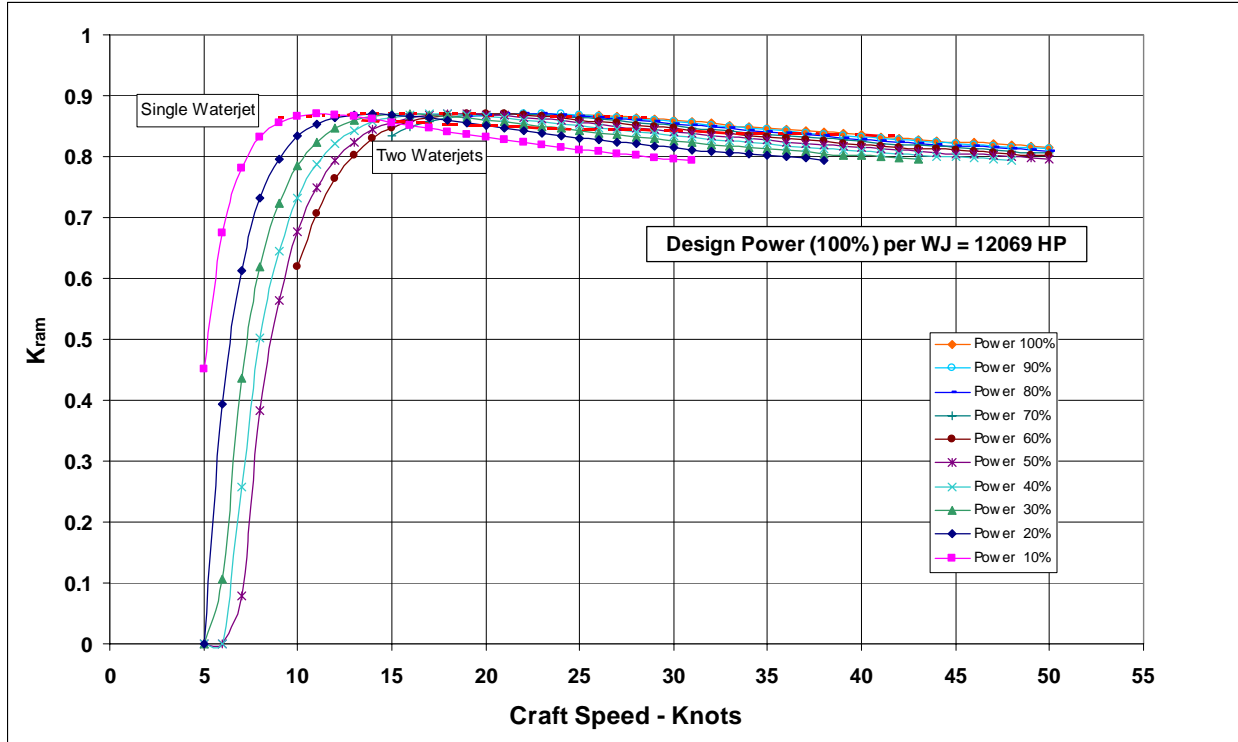


Figure A11. Inlet Loss Coefficient Map versus Speed and Power

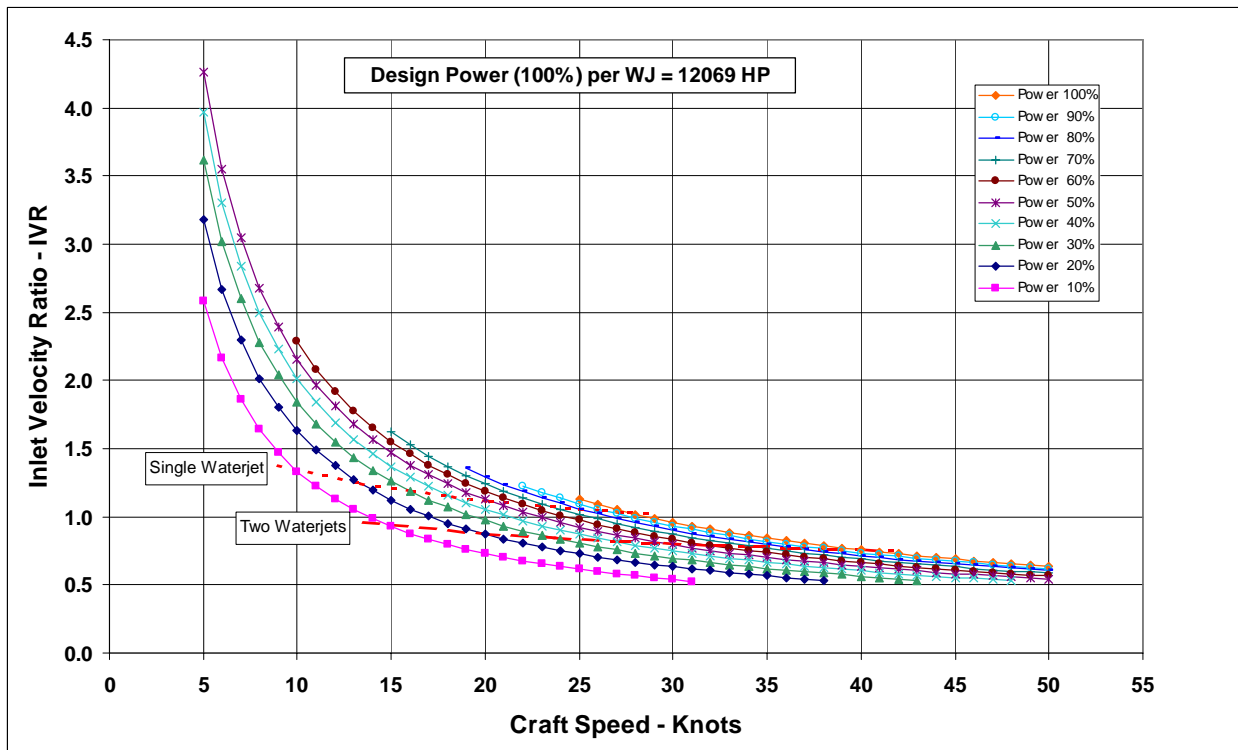


Figure A12. Inlet Velocity Ratio Map versus Speed and Power

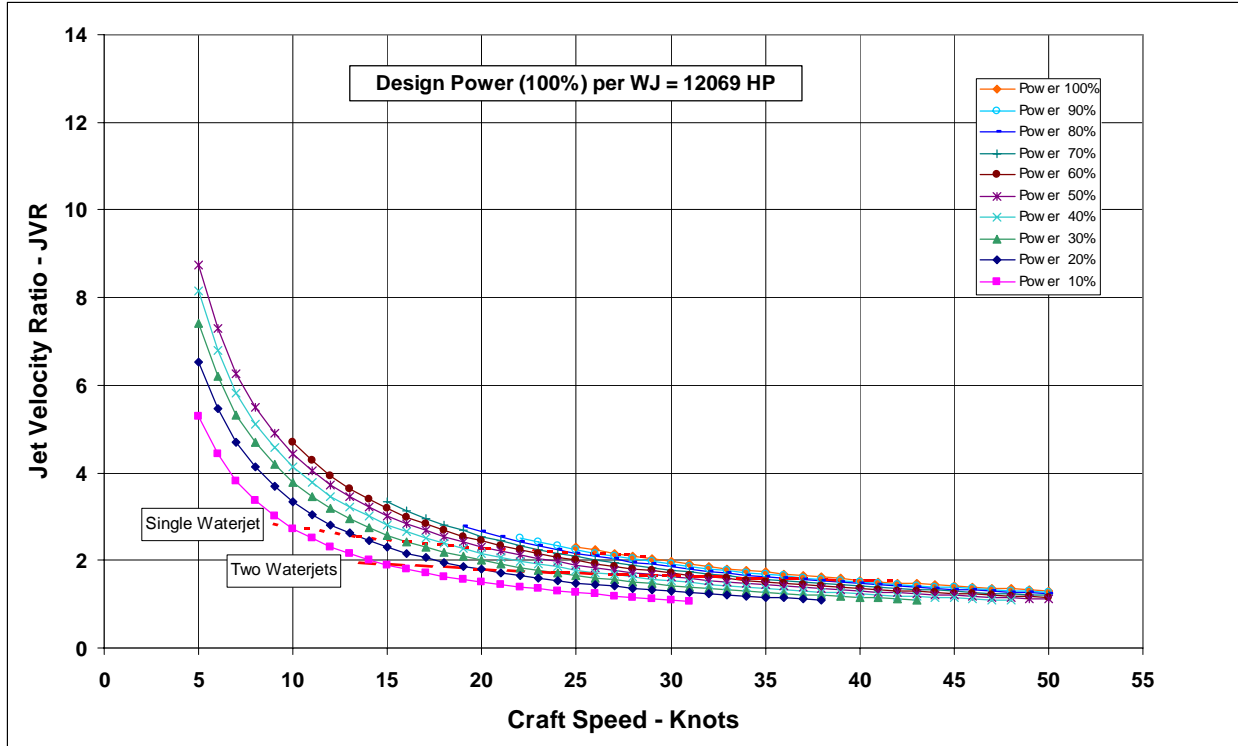


Figure A13. Waterjet Jet Velocity Ratio Map as a Function of Speed and Power